

Supramolecular Polymers

Mechanistic Investigation on Copper–Arylacetylide Polymerization and Sensing Applications

Quanduo Liang, Xiaoyong Chang, Ya-qiong Su, Samuel M. Mugo, and Qiang Zhang*

How to cite:

International Edition: doi.org/10.1002/anie.202100953

German Edition: doi.org/10.1002/ange.202100953

Abstract: Exploration of new polymerization reactions is very intriguing in fundamental and practical research, which will advance reaction theories and produce various functional materials. Herein, we report a new polymerization method based on the reaction of Cu^I and arylacetylide, which generates linear polymers with high molecular weight and low polydispersity index of molecular weight. The Cu–arylacetylide polymerization exhibits different characteristics with traditional polymerizations such as mild reaction temperature, air atmosphere reaction, high molecular weight, fast polymerization rate, and imprecise molar ratio between monomers. The bond formation path and activation energy of each step was investigated by density functional theory calculations to understand the reaction mechanism. The poly(Cu–arylacetylide)s exhibit strong fluorescence emission and inherent semiconductive properties, which have been used to fabricate an electronic device for streptavidin sensing.

Introduction

In the last decade, non-covalent bonds, such as hydrogen bonds, metal coordination, and host-guest interaction, have been used as connecting nodes to synthesize supramolecular polymers, which generate various special properties like self-healing and optoelectronic properties.^[1] As one of the func-

tional polymers, organometallic polymers containing transition metals in either polymer backbones or side chains, differentiate themselves from pure organic polymers with their inherent thermal, magnetic, optical, and electrochemical characteristics.^[2] For example, polymetalloenes containing metalloenes like nickelocene, cobaltocene, and ferrocene in polymer backbones or side chains have been well investigated by Manners, Astruc, and Tang.^[3–5] The cobaltocene and ferrocene allow the polymers electrochemical responses as the transition metals undergo a reversible redox reaction under an electrical field.^[4] Multi-color changes also occur along with the redox reaction, which has potential applications in film manufacture. The electrochemical redox behavior of cobaltocene endowed polycobaltocene good performance as anion-exchange membranes in alkaline fuel cells.^[5] In another case, ruthenium-containing polymers were prepared by Wu and Butt through the coordination reaction of bis(terpyridyl)benzene groups in polymer side chains and ruthenium, which leads to a fast photo-responsive and self-healing properties due to the reversible photocleavage of the Ru–N coordination bonds.^[6] Organometallic polymers are attracting more and more attention as a category of highly-valued materials thanks to their unprecedented qualities with their variety of newfound applications in the field of catalysis, energy, sensing, electronic devices, drug delivery, etc.^[7]

Cu^I and acetylide can form μ,η -coordination bonds leading to charge transfer between them. Much effort has been conducted to prepare Cu^I-alkynyl nanoclusters with photoluminescent properties that have found various applications in organic optoelectronics,^[8] bioimaging,^[9] and catalysis.^[10] The Cu^I-alkynyl nanoclusters were prepared by the reaction of alkyl acetylide or aromatic acetylide with large substituent groups. It has been reported that when the alkyl acetylide was changed to phenyl acetylide, the Cu^I-alkynyl coordination bonds grow in an infinite manner confirmed by X-ray diffraction (XRD).^[11,12] Since the Cu^I-alkynyl complexes are insoluble powder, their structure characterization is limited to XRD. It is impossible to obtain the molecular weight, polydispersity index of molecular weight (PDI), and investigate the dynamics and mechanism of Cu^I-alkynyl polymerization reaction. In addition, owing to the insolubility characteristic of Cu^I-alkynyl complexes, their practical utilization in the development of luminescent coating and electronic devices is still a challenge. It is very intriguing to investigate the Cu^I-alkynyl reaction as a new polymerization method that should be different from traditional polymerization methods like free radical polymerization, anionic polymerization, cationic polymerization, etc. Desirably, the unique fluorescence and conductivity properties of Cu^I-alkynyl polymers are expected due to massive μ,η -coordina-

[*] Q. Liang, Prof. Q. Zhang

State Key Laboratory of Electroanalytical Chemistry, Changchun Institute of Applied Chemistry, Chinese Academy of Sciences Changchun, 130022 (P. R. China) and

School of Applied Chemistry and Engineering, University of Science and Technology of China Hefei, 230026 (P. R. China)

E-mail: qiang.zhang@ciac.ac.cn

X. Chang

Department of Chemistry, Southern University of Science and Technology

Shenzhen, 518055 (P. R. China)

Prof. Y. Su

School of Chemistry, Xi'an Key Laboratory of Sustainable Energy Materials Chemistry, MOE Key Laboratory for Nonequilibrium Synthesis and Modulation of Condensed Matter, State Key Laboratory of Electrical Insulation and Power Equipment, Xi'an Jiaotong University Xi'an, 710049 (P. R. China)

Prof. S. M. Mugo

Department of Physical Sciences, MacEwan University Edmonton, ABT5J4S2 (Canada)

Supporting information and the ORCID identification number(s) for the author(s) of this article can be found under: <https://doi.org/10.1002/anie.202100953>.

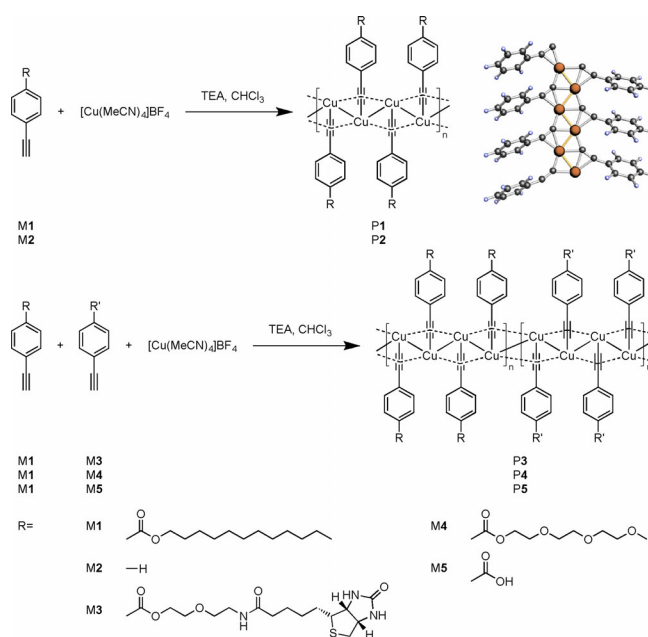
tion bonds. As such, Cu^I-alkynyl polymers are highly amenable for use in applications such as sensing, luminescent coating, electronic devices, etc.

In this submission, we focus on investigating the new polymerization reaction, characterizing the new linear Cu^I-alkynyl polymers, and exploring its applications in electronic devices. Soluble Cu^I-alkynyl polymers were synthesized using long alkyl chains *p*-substituted phenylacetylide. The long alkyl chains overcome the crystallization driving force of Cu^I-alkynyl backbones, which leads to good solubility in organic solvents. Herein, we named the Cu^I-alkynyl compounds as poly(Cu-arylacetylide)s rather than Cu^I-alkynyl complexes due to their linear polymeric characteristics. The molecular weight, PDI, polymerization rate, and the conformation of polymer chains are investigated using various tools and the growth manner of Cu^I-alkynyl backbones was proposed. The experimental results combined with theory simulation provide an insightful understanding of the polymerization reaction mechanism and the ensuing bond formation pathways. We further reveal that this reaction can be used to synthesize a broad library of poly(Cu-arylacetylide)s via homopolymerization or copolymerization using different functional monomers. The poly(Cu-arylacetylide)s distinguish from other traditional organometallic polymers, as its backbone is comprised of μ,η -coordination and Cu–Cu bonds. The special structure allows poly(Cu-arylacetylide)s many unique properties like degradability, fluorescence, and conductivity. Finally, a biosensor was fabricated using biotin containing poly(Cu-arylacetylide) to show the capability of the poly(Cu-arylacetylide)s in electronic devices.

Results and Discussion

Cu–Arylacetylide Polymerization Reaction

The polymerization of **M1** and [Cu(MeCN)₄]BF₄ was carried out with the catalyst of triethylamine (TEA) at room temperature (Scheme 1). The polymerization reaction proceeds to propagate molecular chains via the coordination reaction between alkynyl and Cu¹⁺, which has been verified by infrared spectroscopy (IR, Figure 1a and S1) and ultraviolet spectroscopy (UV, Figure 1b). The peak at 2106 cm⁻¹ in the IR spectrum of **M1** was attributed to the stretching vibration of alkynyl groups, while it shifted to 1927 cm⁻¹ after the polymerization reaction (in the IR spectra of poly(Cu-arylacetylide)s). The UV absorption peak of the benzene group of **M1** was found at 258 nm. When [Cu(MeCN)₄]BF₄ was added to the solution, the intensity of the peak dramatically decreased and a new UV adsorption peak at 484 nm appeared that is attributed to the d- π^* charge transfer (between Cu¹⁺ and alkynyl group), which indicated that coordination bonds formed between the alkynyl group and Cu¹⁺. The chemical structure of the poly(Cu-arylacetylide) has also been characterized using ¹H NMR (Figure S2). To further understand the polymerization reaction, the reaction kinetics was investigated as follows. We found the number-average molecular weight (*M_n*) of poly(Cu-arylacetylide) reached 1 000 000 g mol⁻¹ for 1 min reaction at 20 °C and was



Scheme 1. Synthesis of poly(Cu-arylacetylide)s.

beyond test limitation of gel permeation chromatography (GPC) after 1 min (Figure 1c and S3). When the polymerization reaction was conducted at -20 °C, the *M_n* of 400 000 g mol⁻¹ was obtained after 1 min reaction (Figure 1d). Then, the *M_n* slowly increases plateaus at 800 000 g mol⁻¹ at the terminal stage. Interestingly, the PDI of poly(Cu-arylacetylide) is 1.02 after 60 min, which is even lower than that of some living free-radical polymerizations like atom transfer radical polymerization (ATRP) and reversible addition-fragmentation chain transfer polymerization (RAFT).^[13] The dynamics of the polymerization reaction were measured by monitoring the concentration changes of **M1** with time using a high-performance liquid chromatography-evaporative light scattering detector (HPLC-ELSD) (Figure 1e). The concentration of **M1** dramatically dropped at the beginning of the reaction, and the conversion rate of **M1** slowed down with time. The valence state of Cu in poly(Cu-arylacetylide) has also been investigated using X-ray photoelectron spectroscopy (XPS), as shown in Figure 1f. The peaks at 933.4 eV and 953.2 eV in the spectrum of **P1** were associated with the 2p_{3/2} and 2p_{1/2} of Cu¹⁺ respectively, which slightly shift toward higher binding energy in comparison with [Cu(MeCN)₄]BF₄ (Figure S4). No satellite peaks of Cu²⁺ were observed in the Cu 2p binding energy region indicating Cu covalence state was +1.^[14] No fluorine was found in the XPS spectrum (Figure 1g), which demonstrates the absence of BF₄⁻ in the poly(Cu-arylacetylide)s. The atomic contents ratio of Cu and C is 1:21.2 measured by XPS, respectively, which corresponds to the Cu-arylacetylide molar ratio of 1:1 in **P1**.

The crystal structure of poly(Cu-arylacetylide) was investigated by powder XRD (Figure 1h). The long alkyl chain of **M1** hindered the crystalline behavior of Cu-arylacetylide backbones, which leads to the impossibility of obtaining a high-quality XRD spectrum to reveal the chemical bond parameters of the Cu-arylacetylide backbones. The **M1** was



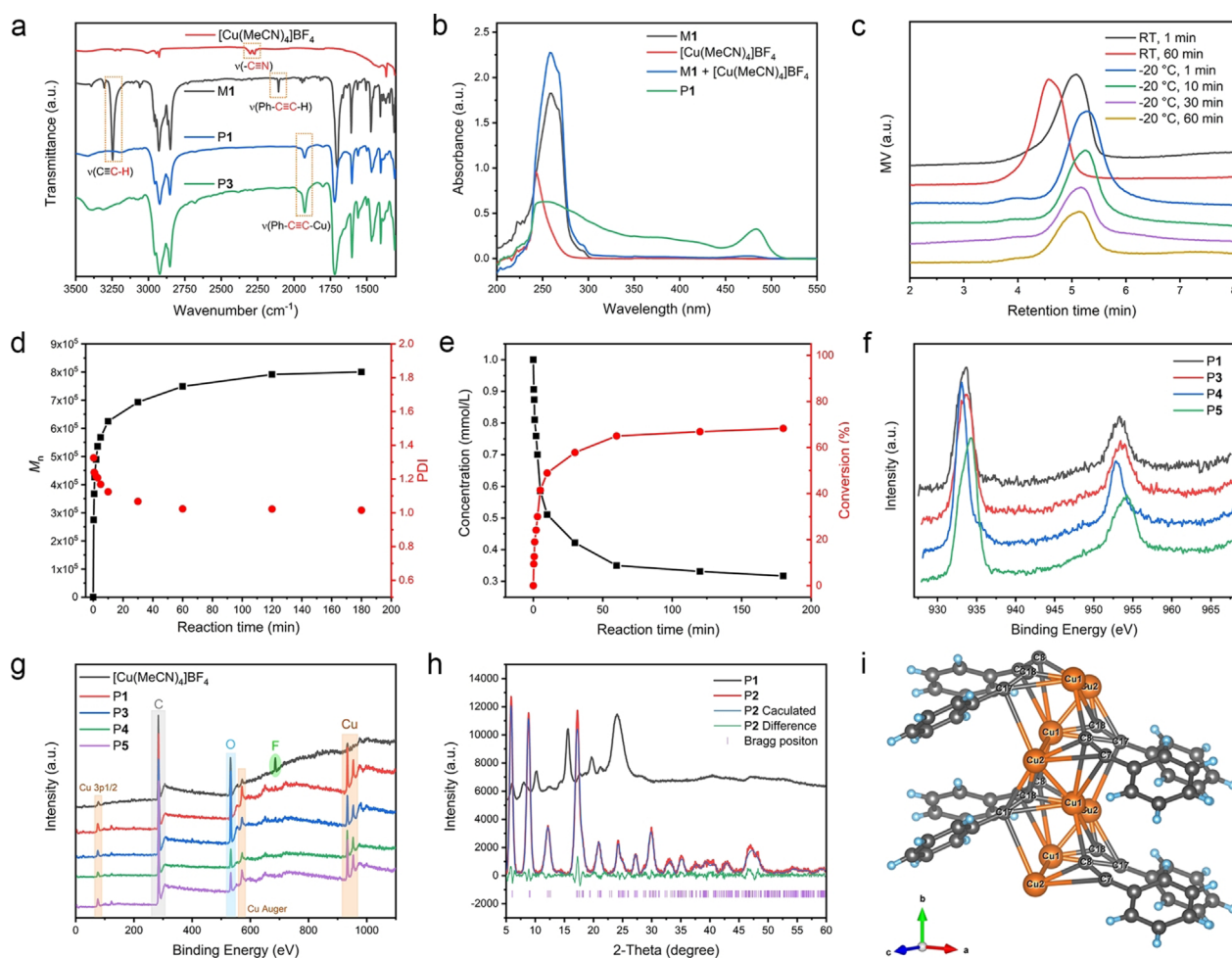


Figure 1. The structure characterization of the poly(Cu-arylacetylide)s and kinetics of polymerization reaction. a) IR spectra of the poly(Cu-arylacetylide)s. b) UV spectra of P1 and the monomers involved in the reaction. c) GPC spectra of P1 for different reaction times. d) M_n and PDI of P1 as a function of reaction time measured by GPC. e) Concentration of the monomer (M1) as a function of reaction time measured by HPLC-UV. f) XPS analysis of copper in $[\text{Cu}(\text{MeCN})_4]\text{BF}_4$ and P1. g) XPS full spectra of $[\text{Cu}(\text{MeCN})_4]\text{BF}_4$ and the poly(cu-arylacetylide)s. h) XRD patterns of P1, P2, and Rietveld profile refinement plot of P2. i) Crystal structure of P2.

replaced by phenylacetylene (M2) to synthesize crystal poly(Cu-phenylacetylide) (P2) for structure investigation. The XRD spectrum of P2 was subjected to the Rietveld profile refinement by using the General Structure Analysis System (GSAS) program according to the structure of CCDC-242490.^[12,15] The crystal structure and crystallographic data of P2 have been shown in Figure 1i and Table 1, respectively. P2 belongs to the monoclinic system and the space group is $P2_1$. Viewed along the b axis, every four Cu atoms form a period of the spiral ascending structure, and phenylacetylenes are distributed around the Cu-Cu long chain. Refined Cu-Cu distances are 2.45–2.65 Å (Table S1), while the Cu-C distances are 1.64–2.60 Å. The distance between Cu atoms is smaller than the van der Waals radius of copper, which indicates the existence of weak interaction between joint Cu atoms and the formation of coordination bonds between Cu and phenylacetylene.^[16] It can be observed that the XRD pattern of P1 bulges in the 2θ range of 15–30°, which indicates the existence of amorphous components in P1. Indexing the XRD peak positions of P1 gave triclinic cell parameters, and P1 exhibited a larger unit cell volume than P2

(Table 1). Density functional theory (DFT) calculations were conducted to optimize the crystal structures of P1 and P2 and the corresponding CIF files have been provided in Supporting Information (SI, Data S1 and S2) and The Cambridge Crystallographic Data Centre (CCDC, 2061812 and 2061813). The optimized lattice parameters of P1 and P2 are listed in Table 1. The calculation result of P2 is in good agreement with the result of XRD refinement, while a deviation between the diffraction result and the calculation result of P1 was found due to the presence of amorphous structures in P1. Nevertheless, in the simulated P1 structure, the arrangement of Cu and C atoms is consistent with that in P2 (Figure S5). The information on bond lengths and angles are beneficial to understand the stereochemical structure of poly(Cu-phenylacetylide)s.

Polymerization Mechanism

To further explore the polymerization mechanism, DFT calculation was applied to investigate the bond formation

Table 1: Cell parameters for powder structure P1 and P2.

| | P1 ^[a] | P2 ^[b] | P1 ^[c] | P2 ^[d] |
|-----------------------------|-------------------|-------------------|-------------------|-------------------|
| Crystal system | Triclinic | Monoclinic | Triclinic | Monoclinic |
| Space group | P1 | P21 | P1 | P21 |
| <i>a</i> [Å] | 24.406 | 15.4(2) | 44.441 | 15.2659 |
| <i>b</i> [Å] | 23.674 | 5.174(7) | 4.97866 | 3.78946 |
| <i>c</i> [Å] | 11.733 | 10.366(9) | 9.5497 | 9.7428 |
| α [°] | 84.5 | 90(0) | 89.3079 | 90 |
| β [°] | 140.8 | 108.5(1) | 125.708 | 111.561 |
| γ [°] | 83.3 | 90(0) | 92.0842 | 90 |
| <i>V</i> [Å ³] | 4105.0 | 783.3(103) | 1714.463 | 524.18 |
| χ^2 ^[d] | – | 1.59 | – | – |
| R_{wp} [%] ^[e] | – | 14.62 | – | – |
| R_p [%] ^[f] | – | 9.832 | – | – |

[a] Unit cell parameters obtained by indexing peak positions of diffraction patterns using Jade 6 program. [b] Crystallographic parameters obtained from Retveld refined results. [c] Crystallographic parameters obtained from DFT calculation results. [d] $\chi^2 = \sum_i w_i (y_{i,0} - y_{i,c})^2 / (N_{obs} - N_{var})$. [e] $R_p = \sum_i |y_{i,0} - y_{i,c}| / \sum_i |y_{i,0}|$. [f] $R_{wp} = |\sum_i w_i (y_{i,0} - y_{i,c})^2 / \sum_i w_i (y_{i,0})^2|^{1/2}$ in which $y_{i,0}$ and $y_{i,c}$ are the observed and calculated intensities at point *i* of the profile, respectively. N_{obs} is the number of theoretical Bragg peaks in the 2θ range considered. N_{var} is number of the refined parameters. Statistical weights w_i are normally taken as $1/y_{i,0}$.^[12]

path and its corresponding potential barrier (SI, Data S3). P2 was selected for the mechanism investigation due to its simple chemical structure that can reduce computation load. To this end, a theoretical model was constructed containing a short Cu-phenylacetylene oligomer, a Cu¹⁺ ion, and a free phenylacetylene monomer (Figure 2). The Cu¹⁺ ion and phenylacetylene spontaneously reacted to form a Cu-phenylacetylene complex. The Cu-phenylacetylene complex got close to the Cu-phenylacetylene oligomer from a far distance and finally inserted into the Cu-phenylacetylene oligomer. The bond formation process and activation energy of each step have been shown in Figure 2. As the distance between the monomer and the oligomer became shorter, the benzene rings on the oligomer chain rotate to minimize system energy. When the Cu...C distance is 2.1 Å, a Cu-C coordination bond formed between the Cu¹⁺ and the phenyl unit of the oligomer.

As the monomer continued to approach the oligomer chain, the σ bond was replaced by a new coordination bond between Cu and alkynyl group due to the steric effect of the benzene ring hindering the rotation of the molecular chain. When the distance between Cu atoms is shorter than 2.7 Å, it leads to the formation of Cu-Cu interaction. When the monomer is completely inserted into the oligomer, the molecular chain continued to twist, arrange, and form a stable configuration (SI, Movie S1). The polymerization reaction is a thermodynamically favorable process with an energy downhill of 3.68 eV. The required largest activation energy is only 0.17 eV.

The polymerization reaction can also take place in the manner of interfacial polymerization. As shown in Figure 3a, two immiscible solvents (hexane and acetonitrile) were used to dissolve M1/TEA (in hexane) and [Cu(MeCN)₄]BF₄ (in acetonitrile). When the two solutions came into contact at room temperature, a film formed on the interface within

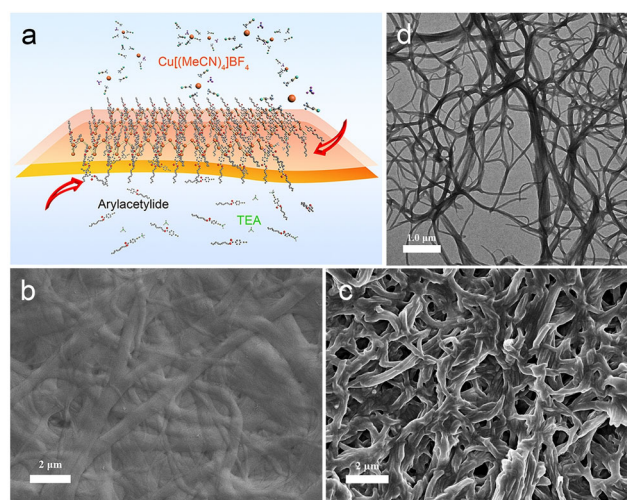


Figure 3. a) Schematic diagram of P1 synthesized by interfacial polymerization. b) SEM image of P1 film prepared by interfacial polymerization. c) SEM image of P1 film prepared by solution-casting. d) TEM images of P1.

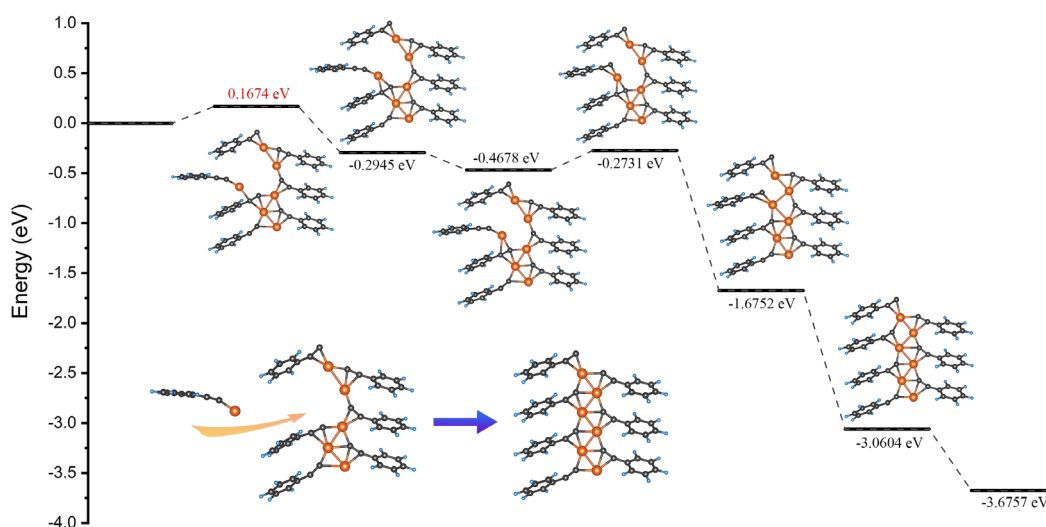


Figure 2. DFT simulation of the Cu-arylacetylide polymerization reaction.



2 min. The M_n and PDI were $2.61 \times 10^4 \text{ g mol}^{-1}$ and 1.35 measured by GPC, respectively. This result demonstrates that the Cu-arylacetylide polymerization reaction does not require a precise molar ratio of reactants. Interfacial polymerization is a powerful tool to prepare ultra-thin membranes on substrate surfaces. For example, interfacial polymerization has been demonstrated in preparing polyamide reverse osmotic membranes using trimesoyl chloride and 1,2-phenylenediamine.^[17] Thus the Cu-arylacetylide polymerization reaction offers potentials for the preparation of ultra-thin membranes and functionalization of substrate surfaces. To explore the tolerance of the reaction, arylacetylide with biotin groups (M2), PEO (M3), and -COOH were synthesized and used to copolymerize with M1. A series of poly(Cu-arylacetylide)s with biotin groups (P3), PEO (P4), and -COOH (P5) have been successfully synthesized with M_n of $5.96 \times 10^4 \text{ g mol}^{-1}$ for P3, $6.87 \times 10^4 \text{ g mol}^{-1}$ for P4, and $4.97 \times 10^4 \text{ g mol}^{-1}$ for P5 at -20°C , which indicates that the Cu-arylacetylide polymerization reaction can tolerate various polar groups. Therefore, the Cu-arylacetylide polymerization reaction can be used to prepare various materials with desirable properties. For example, the biotin can form strong non-covalent interactions with streptavidin with a dissociation constant of $10^{-15} \text{ mol L}^{-1}$. Streptavidin has been widely used to tag proteins for signal amplification in immunoassay.^[18] Therefore, the P3 can be used to recognize streptavidin-conjugated biomolecules through the streptavidin-biotin binding. It can be concluded that the Cu-arylacetylide polymerization distinguishes other polymerization methods with the following distinctive characteristics: (i) mild reaction temperature (-20°C to 30°C), (ii) air atmosphere reaction without protecting gas, (iii) high molecular weight ($M_n > 1000000$), (iv) low PDI ($\text{PDI} < 1.1$), (v) fast polymerization

rate, (vi) imprecise molar ratio between monomers, (vi) tolerance of various polar and functional groups.

Investigation on Morphology, Mechanical Properties, Water Contact Angles, and Stability of Poly(Cu-arylacetylide)s

The morphologies of the poly(Cu-arylacetylide)s have been investigated using SEM and TEM (Figure 3b–d and Figure S, 6, 7). When the reaction was conducted in strong polar solvents or the poly(Cu-arylacetylide)s were treated using strong polar solvents like methanol, ethanol, acetone, the poly(Cu-arylacetylide)s self-assembled into fibers with a length of tens μm . When the Cu-arylacetylide polymerization reaction occurred in medium polar solvents or the poly(Cu-arylacetylide)s were dissolved in medium polar solvents like chloroform or hexafluoroisopropanol, smooth and dense films were obtained by the methods of spin-coating or solution-casting (Figure S8). The contact angle test of the film shows that the water contact angle of P1 is 108.2° (Figure S9). P3–P5 exhibit lower water contact angles (95.9° for P3, 102.3° for P4, and 98.5° for P5) in comparison to P1 as a result of introducing the hydrophilic substituent groups.

Nanoindentation tests were employed to investigate the mechanical properties of the poly(Cu-arylacetylide) films (Figure 4a). The hardness and elastic modulus of the poly(Cu-arylacetylide)s were in the range of 92.36–197.76 MPa and 3.30–8.42 GPa, respectively (Table S2), which are associated with M_n and intermolecular interaction. The P3 exhibited the highest hardness and modulus due to the hydrogen bonds between biotin groups. The thermal stability of poly(Cu-arylacetylide)s has been studied by thermogravimetric analysis (TGA), which exhibited a two steps degradation process

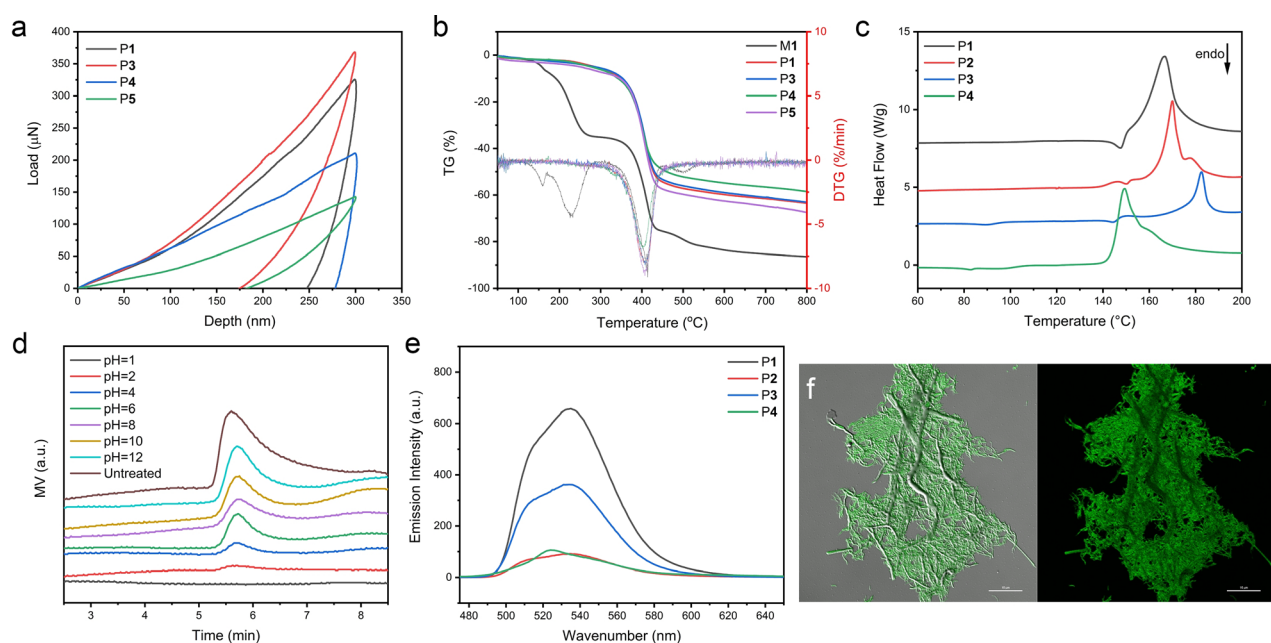


Figure 4. Characterization of mechanical, thermal, and fluorescent properties of the poly(Cu-arylacetylide)s. a) Indentation load-depth responses of the poly(Cu-arylacetylide)s. b) TGA thermograph of the poly(Cu-arylacetylide)s. c) DSC curves of the poly(Cu-arylacetylide)s. d) GPC curves of the poly(Cu-arylacetylide)s after being treated by solution with different pH. e) Fluorescence emission spectra of the poly(Cu-arylacetylide)s. f) Confocal micrographs of P1.

at 250°C and 400°C, respectively (Figure 4b). The first weight loss of around 250°C resulted from the degradation of ester groups.^[19] The second weight loss of around 400°C was associated with the degradation of polymer backbones. In the comparison of **M1**, the thermal stability of poly(Cu-arylacetylide)s was greatly enhanced, and higher residual masses (40–60%) were observed due to the presence of Cu in these polymers. Differential scanning calorimetry (DSC) has been utilized to characterize the thermal behavior of the poly(Cu-arylacetylide)s (Figure 4c). A melting peak in the range of 140–152°C was observed, and the melting enthalpy of 16.64 J g⁻¹ for **P1** was obtained which was calculated from the DSC result. In addition, crystallization peaks near 160°C were also observed, which corresponded to the crystallization of copper-alkyne backbones, and corresponding crystallization enthalpies for **P1**, **P3**, **P4**, and **P5** were 260.6, 169.0, 136.3, and 208.5 J g⁻¹, respectively. The stability of **P1** in acidic and basic environments was also tested by monitoring the changes in molecular weight via GPC. The **P1** was treated by aqueous solutions of pH 1–12 for 1 h and the corresponding GPC curves were shown in Figure 4d. The **P1** is stable in the weak acidic, neutral, and basic environment (pH > 4). It starts to degrade into **M1** and a small number of other products at the solutions of pH < 4, which has been verified by gas chromatography-mass spectrometry (GC-MS, Figure S10) and ¹H NMR (Figure S11). When the **P1** was treated by a solution of pH 1 for 1 h, it completely degraded into small molecules and no high molecular weight polymer was detected by GPC. The acid-degradable property for poly(Cu-arylacetylide)s lend it to applications as a controlled drug delivery carrier. For example, cancer progression, inflammation, and immune dysfunctions generate acidic microenvironments that may trigger the degradation of poly(Cu-arylacetylide)s.^[20] After 2 months of storage in the air and room temperature environment, no changes in chemical structures and *M_n* indicating the good stability of poly(Cu-arylacetylide)s (Figure S12).

Fluorescent Property of Poly(Cu-arylacetylide)s

It has been reported that some Cu^I clusters exhibit strong fluorescence emission, comparable to Ir^{III} complexes.^[21] However, stability is a great challenge due to the d10 closed electronic configuration of Cu^I.^[22] In this study, the fluorescence of poly(Cu-arylacetylide)s has been investigated and the results have been shown in Figure 4e. Poly(Cu-arylacetylide)s exhibits fluorescence properties in a wide range of excitation light wavelengths (300–560 nm, 650–800 nm) (Figure S13). When the **P1** was irradiated by 460 nm wavelength light in chloroform, it exhibited two emission peaks at 515 nm and 535 nm, respectively. The emission peaks at 490–550 nm are attributed to a metal-perturbed ligand-centered π - π^* (acetylide) emission, from metal-to-ligand or ligand-to-metal charge transfer transitions.^[12] It has been observed that the biotin and carboxyl groups in the poly(Cu-arylacetylide)s led to decreases in the fluorescence intensity, which is also found in other electron deficient acetylide complexes.^[23] The introduction of polar groups will cause a decrease in the

fluorescence intensity of the poly(Cu-arylacetylide)s. In addition, when **P1** is dispersed in a polar solvent (Figure S14), the emission peaks exhibit a blue shift (Figure S15). The strong fluorescence of **P1** was also observed by a fluorescent confocal microscope, as shown in Figure 4f. To better understand the fluorescent performance of poly(Cu-arylacetylide)s, the decay behavior of **P1** photoexcited carriers was investigated. The decay lifetime of carriers in **P1** is approximately 64.78 ns (Figure S16), which indicates good separation efficiency of photoexcited charges and allows poly(Cu-arylacetylide)s to find potential applications as photocatalysts. After storage in the air atmosphere for 2 months, no distinct loss in fluorescence intensity and UV absorption was observed, which demonstrates that the fluorescence performance stability of Cu^I was greatly enhanced in the linear polymer (Figure S17 and S18). The high stability was attributed to the electron transfer from arylacetylide to Cu^I in the poly(Cu-arylacetylide)s.

Conductive Property and Application of Biotin Containing Poly(Cu-arylacetylide)

The conductive performance of poly(Cu-arylacetylide)s is expected, as they are comprised of Cu-Cu bonds and Cu-acetylide coordination bonds. Figure S19 shows the current-voltage (*I*-*V*) curves of **P3** in the voltage range of -30 V to 30 V. A conductivity of 1.96×10^{-5} S cm was observed indicating that **P3** is a kind of typical semiconductors. The *I*-*V* curves exhibited excellent linear characteristics, which demonstrate the typical Ohmic behavior and constant conductivity. The semi-conductive performance allows the poly(Cu-arylacetylide)s to find applications in electronic sensors. Herein, a streptavidin sensor was prepared using a silver interdigital electrode coated by **P3** to demonstrate biosensing applications (Figure 5a). The interaction between streptavidin and biotin has been reported as one of the strongest non-covalent interactions in nature with a dissociation constant on the order of $\approx 10^{-15}$ mol L⁻¹.^[24] The streptavidin is broadly used to conjugate with biomolecules for immunoassay and biomolecular recognition. The response of the sensor to streptavidin in artificial urine and real urine samples was investigated. The current of the sensor decreased rapidly and finally stabilized with increasing the streptavidin amount (Figure 5b). The current of the sensor did not change significantly when the artificial urine or real urine was free of streptavidin, while it shows a 90% decrease when the streptavidin concentration increases from 0 to 3 μ M (Figure 5c). The changes in current are attributed to the variation of molecular chain conformation caused by streptavidin, which distorts the electron transfer channels and leads to a resistance increase of **P3** (Figure 5d). The limit of detection of the sensor was obtained as 35.0 nM, which is much higher than that (2.5 mg mL⁻¹) of Au nanoparticles/hydrogel composites reported by others.^[25] Therefore, the sensor has the potential for biosensing applications in a urine environment.



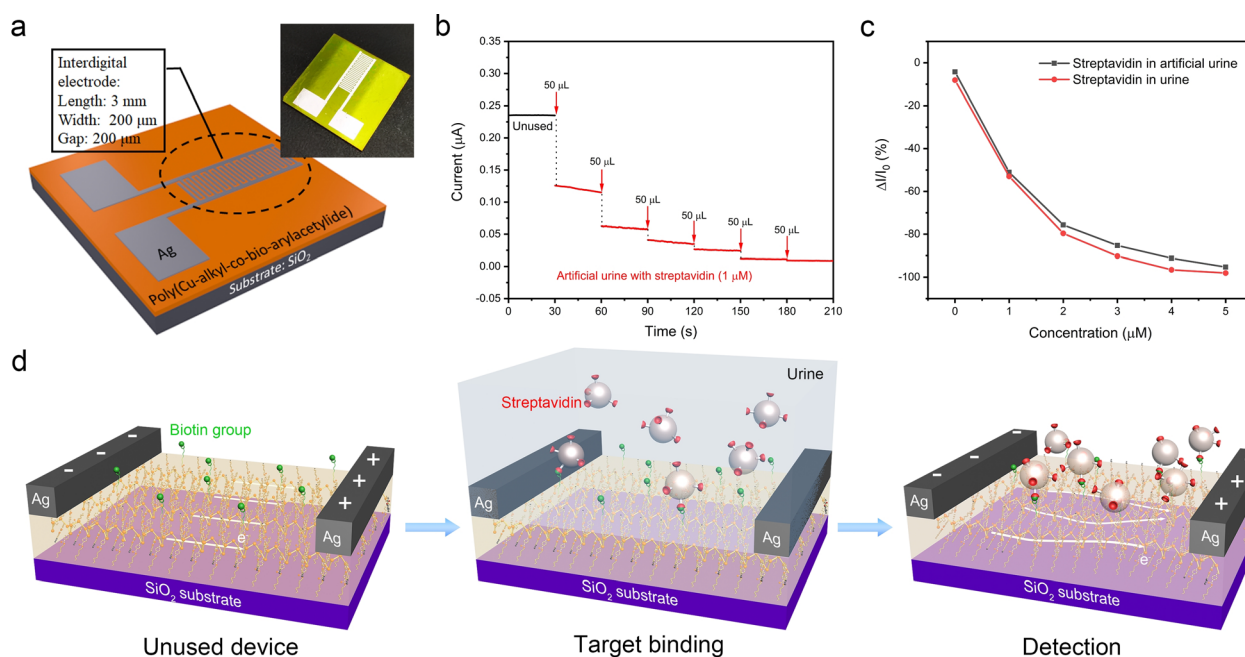


Figure 5. Poly(Cu-arylacetylide)-based sensor for streptavidin detection. a) Schematic diagram and an optical picture of the poly(Cu-arylacetylide)-based streptavidin sensor. b) Current response with time upon exposure to streptavidin. c) The current response of the device to streptavidin concentration in artificial urine and real urine. d) The strategy of the poly(Cu-arylacetylide)-based sensor to detect streptavidin.

Conclusion

In summary, the poly(Cu-arylacetylide)s were synthesized upon the polymerization reaction of Cu^{I} complex and acetylide. The copper-arylacetylide polymerization reaction is different from the traditional polymerization methods. It has the characteristics of mild reaction conditions, a fast reaction rate, and no need for protective gas. In addition, the produced poly(Cu-arylacetylide)s have a high molecular weight and a narrow molecular weight distribution without precise control of the feed ratio. It has characteristics similar to living polymerization but has easier reaction conditions in comparison. The tolerance of the poly(Cu-arylacetylide) makes it possible to introduce functional monomers into the main chain and achieve specific sensing functions. The poly(Cu-arylacetylide) exhibit strong fluorescence emission, good fluorescence stability, and a long decay lifetime. The conductive performance was observed, which allow the poly(Cu-arylacetylide) to fabricate biosensors. The sensors show the ability to sense streptavidin in the urine. This novel polymerization method and the unique properties of poly(Cu-arylacetylide)s exhibit profound research significance and broad future application prospects.

Acknowledgements

The authors gratefully acknowledge the funding from the International Cooperation Project of Jilin Province Science and Technology Development Plan (20200801008GH) and the National Key Research and Development Program of China (2018YFD1100503).

Conflict of interest

The authors declare no conflict of interest.

Keywords: copper-arylacetylide polymerization · DFT calculations · poly(Cu-arylacetylide) · stimuli-responsive polymers · supramolecular polymers

- [1] a) T. Aida, E. W. Meijer, S. I. Stupp, *Science* **2012**, *335*, 813–817; b) M. Burnworth, L. Tang, J. R. Kumpfer, A. J. Duncan, F. L. Beyer, G. L. Fiore, S. J. Rowan, C. Weder, *Nature* **2011**, *472*, 334–337.
- [2] a) T. Zhu, Y. Sha, J. Yan, P. Pageni, M. A. Rahman, Y. Yan, C. Tang, *Nat. Commun.* **2018**, *9*, 4329; b) Y. Wang, D. Astruc, A. S. Abd-El-Aziz, *Chem. Soc. Rev.* **2019**, *48*, 558–636; c) V. M. Santhini, O. Stetsovych, M. Ondráček, J. I. Mendieta Moreno, P. Mutombo, B. Torre, M. Švec, J. Klívar, I. G. Stará, H. Vázquez, et al., *Adv. Funct. Mater.* **2021**, *31*, 2006391.
- [3] H. Gu, R. Ciganda, P. Castel, S. Moya, R. Hernandez, J. Ruiz, D. Astruc, *Angew. Chem. Int. Ed.* **2018**, *57*, 2204–2208; *Angew. Chem.* **2018**, *130*, 2226–2230.
- [4] R. A. Musgrave, A. D. Russell, D. W. Hayward, G. R. Whittell, P. G. Lawrence, P. J. Gates, J. C. Green, I. Manners, *Nat. Chem.* **2017**, *9*, 743–750.
- [5] T. Zhu, Y. Sha, H. A. Firouzjaie, X. Peng, Y. Cha, D. M. M. M. Dissanayake, M. D. Smith, A. K. Vannucci, W. E. Mustain, C. Tang, *J. Am. Chem. Soc.* **2020**, *142*, 1083–1089.
- [6] a) W. Sun, Y. Wen, R. Thiramanas, M. Chen, J. Han, N. Gong, M. Wagner, S. Jiang, M. S. Meijer, S. Bonnet, et al., *Adv. Funct. Mater.* **2018**, *28*, 1804227; b) J. Liu, C. Xie, A. Kretzschmann, K. Koynov, H.-J. Butt, S. Wu, *Adv. Mater.* **2020**, *32*, 1908324.
- [7] a) Q. Dong, Z. Meng, C. Ho, H. Guo, W. Yang, I. Manners, L. Xu, W. Wong, *Chem. Soc. Rev.* **2018**, *47*, 4934–4953; b) M. Gallei, C. Rüttiger, *Chem. Eur. J.* **2018**, *24*, 10006–10021; c) Z. Ruan, Z. Li, *Polym. Chem.* **2020**, *11*, 764–778; d) H. Zhou, M.



- Chen, Y. Liu, S. Wu, *Macromol. Rapid Commun.* **2018**, *39*, 1800372.
- [8] a) P. Yuan, R. Chen, X. Zhang, F. Chen, J. Yan, C. Sun, D. Ou, J. Peng, S. Lin, Z. Tang, et al., *Angew. Chem. Int. Ed.* **2019**, *58*, 835–839; *Angew. Chem.* **2019**, *131*, 845–849; b) E. Fresta, J. Fernández-Cestau, B. Gil, P. Montaña, J. R. Berenguer, M. T. Moreno, P. B. Coto, E. Lalinde, R. D. Costa, *Adv. Opt. Mater.* **2020**, *8*, 1901126.
- [9] M. Zhang, X. Dong, Z. Wang, H. Li, S. Li, X. Zhao, S. Zang, *Angew. Chem. Int. Ed.* **2020**, *59*, 10052–10058; *Angew. Chem.* **2020**, *132*, 10138–10144.
- [10] H. Jiang, P. Zhou, Y. Wang, R. Duan, C. Chen, W. Song, J. Zhao, *Adv. Mater.* **2016**, *28*, 9776–9781.
- [11] X. Chang, K. Low, J. Wang, J. Huang, C. Che, *Angew. Chem. Int. Ed.* **2016**, *55*, 10312–10316; *Angew. Chem.* **2016**, *128*, 10468–10472.
- [12] S. S. Y. Chui, M. F. Y. Ng, C. Che, *Chem. Eur. J.* **2005**, *11*, 1739–1749.
- [13] a) K. Matyjaszewski, J. Xia, *Chem. Rev.* **2001**, *101*, 2921–2990; b) W. A. Braunecker, K. Matyjaszewski, *Prog. Polym. Sci.* **2007**, *32*, 93–146.
- [14] Z. Guan, W. Luo, J. Feng, Q. Tao, Y. Xu, X. Wen, G. Fu, Z. Zou, *J. Mater. Chem. A* **2015**, *3*, 7840–7848.
- [15] H. M. Rietveld, *J. Appl. Crystallogr.* **1969**, *2*, 65–71.
- [16] Z. Wei, J. Hu, K. Zhu, W. Wei, X. Ma, Y. Zhu, *Appl. Catal. B* **2018**, *226*, 616–623.
- [17] S. Lim, H. van Tran, N. Akther, S. Phuntsho, H. K. Shon, *J. Membr. Sci.* **2019**, *586*, 281–291.
- [18] Y. Chen, W. Chien, D. Lee, K. Tan, *Anal. Chem.* **2019**, *91*, 12461–12467.
- [19] D. K. Chattopadhyay, D. C. Webster, *Prog. Polym. Sci.* **2009**, *34*, 1068–1133.
- [20] V. Huber, C. Camisaschi, A. Berzi, S. Ferro, L. Lugini, T. Triulzi, A. Tuccitto, E. Tagliabue, C. Castelli, L. Rivoltini, *Semin. Cancer Biol.* **2017**, *43*, 74–89.
- [21] M. Hashimoto, S. Igawa, M. Yashima, I. Kawata, M. Hoshino, M. Osawa, *J. Am. Chem. Soc.* **2011**, *133*, 10348–10351.
- [22] J. Yang, Z. Li, Q. Jia, *Sens. Actuators B* **2019**, *297*, 126807.
- [23] V. W. Yam, W. K. Fung, K. Cheung, *J. Cluster Sci.* **1999**, *10*, 37–69.
- [24] T. Sano, C. R. Cantor, *J. Biol. Chem.* **1990**, *265*, 3369–3373.
- [25] J. de Oliveira, J. Monteiro, P. Buzzetti, B. Cabral Júnior, E. Radovanovic, E. Giroto, *J. Braz. Chem. Soc.* **2020**, *31*, 1771–1777.

Manuscript received: January 20, 2021

Accepted manuscript online: February 8, 2021

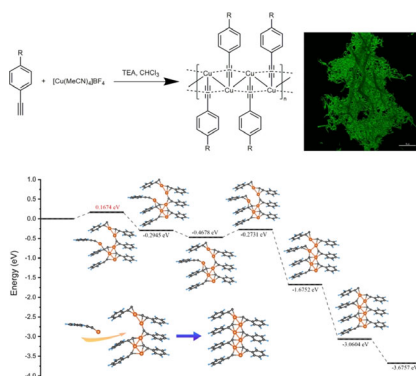
Version of record online: ■ ■ ■ ■ ■ ■ ■ ■ ■ ■

Research Articles

Supramolecular Polymers

Q. Liang, X. Chang, Y. Su, S. M. Mugo,
Q. Zhang*     

Mechanistic Investigation on Copper–
Arylacetylide Polymerization and Sensing
Applications



For the first time, a copper–arylacetylide polymerization exhibiting the characteristics of mild reaction temperature, air atmosphere reaction, high molecular weight, and fast polymerization rate is presented. DFT calculations show that the polymerization is a thermodynamically favorable process. The resulting polymers exhibit strong fluorescence emission and inherent semiconductive properties.